Hybridization and anisotropy in the exchange interaction in three-dimensional Dirac semimetals

D. Mastrogiuseppe,[1,2] N. Sandler,[1] and S. E. Ulloa[1]

[1]*Department of Physics and Astronomy, and Nanoscale and Quantum Phenomena Institute, Ohio University, Athens, Ohio 45701-2979, USA*

[2]*Instituto de Física Rosario (CONICET), 2000 Rosario, Argentina*

(Received 5 December 2015; revised manuscript received 13 March 2016; published 28 March 2016)

We study the Ruderman-Kittel-Kasuya-Yosida interaction in three-dimensional Dirac semimetals. Using retarded Green's functions in real space, we obtain and analyze asymptotic expressions for the interaction, with magnetic impurities at different distances and relative angle with respect to high symmetry directions on the lattice. We show that the Fermi velocity anisotropy in these materials produces a strong renormalization of the magnitude of the interaction, as well as a correction to the frequency of oscillation in real space. Hybridization of the impurities to different conduction electron orbitals are shown to result in interesting anisotropic spin-spin interactions which can generate spiral spin structures in doped samples.

DOI: 10.1103/PhysRevB.93.094433

I. INTRODUCTION

Dirac semimetals are fascinating new materials that can be considered analogs of graphene in three dimensions. They possess robust Dirac points that are protected by crystalline symmetry, and strong spin-orbit interaction (SOI). Na_3Bi and Cd_3As_2 are among these compounds, where the unconventional Dirac character was detected in angle resolved photoemission and transport experiments [1–5]. Many more materials have been proposed as promising candidates [6]. When time-reversal or inversion symmetry is broken, the degeneracy of each Dirac cone splits without the opening of a gap, leading to the Weyl semimetal phase. The latter phase is characterized by unconventional properties, such as a chiral anomaly and Fermi arcs on the surfaces, as recently measured in TaAs [7–9], NbAs [10], and NbP [11]. These unusual properties suggest that magnetic impurities can reveal exotic behavior, as predicted, for instance, for the Kondo effect [12–14].

Impurities are ubiquitous in the preparation of experimental samples and they can also be purposely introduced by different processes. It is well known that in metallic hosts, magnetic impurities interact effectively through the electron gas, and that this interaction has an oscillatory decay when the separation between them is increased. This Ruderman-Kittel-Kasuya-Yosida (RKKY) interaction [15–17] gets more complicated when the host material has a more involved band structure and/or additional degrees of freedom. For instance, graphene is predicted to have an unconventional decay dependence for the charge neutral case [18,19]. Strong SOI can also affect the behavior, giving rise to spin-spin interactions that contain anisotropic terms such as Ising and Dzyaloshinskii-Moriya (DM) interactions on top of the usual Heisenberg-like terms [20].

In this work we study the RKKY interaction in three-dimensional (3D) Dirac semimetals, focusing on Na_3Bi and Cd_3As_2, two compounds with strong Fermi velocity anisotropy [1,3]. Starting with a low energy model, we consider magnetic impurities that hybridize with Na-s and Bi-p orbitals, the most relevant near the band crossings that build the Dirac points [21]. We obtain asymptotic expressions for the interaction, and analyze its behavior as a function of the impurity separation as related to the underlying lattice. The role of the SOI in these materials manifests uniquely when each impurity hybridizes with a different conduction electron orbital, resulting in strong interaction anisotropies. We also show that Dirac dispersion anisotropies seen in these materials have strong impact on the amplitude and spatial dependence of the effective exchange interaction.

II. MODEL

Two magnetic impurities coupled to an electron gas can be described by the Hamiltonian

$$H = H_0 + J \sum_{j=1,2} \boldsymbol{S}_j \cdot \boldsymbol{s}(\boldsymbol{R}_j), \tag{1}$$

where H_0 is the unperturbed Hamiltonian for the host material, $\boldsymbol{s}(\boldsymbol{r}) = \sum_i \delta(\boldsymbol{r} - \boldsymbol{r}_i)\boldsymbol{\sigma}_i$, in units of $\frac{\hbar}{2}$, is the spin density operator for the conduction electrons, where $\boldsymbol{r}_i$ and $\boldsymbol{\sigma}_i$ are the position and Pauli matrices for electron i. $\boldsymbol{S}_j$ is the localized spin operator for impurity j. At second order in perturbation theory in the interaction parameter J, one can obtain an effective Hamiltonian that describes the carrier mediated interaction between the impurities separated by a distance vector $\boldsymbol{R}$

$$H_{\mathrm{RKKY}} = J^2 \sum_{\mu,\mu'} S_1^{\mu}\, \chi_{\mu,\mu'}(\mathbf{R})\, S_2^{\mu'}, \tag{2}$$

where $\chi_{\mu,\mu'}$ is the static spin susceptibility tensor of the electron gas, and μ,μ' represent the Cartesian components [22]. For conventional electron gases, and in the absence of SOI, the susceptibility tensor is diagonal so that the effective spin-spin coupling is isotropic. Moreover, the interaction decays as $|\mathbf{R}|^{-D}$, where D is the dimensionality of the system [23]. When the SOI is present, anisotropic components of Ising and/or DM type may appear [20]. Additionally, the presence of particular features in the band structure, such as Dirac points, may change the decay exponent (e.g., in graphene, $|\mathbf{R}|^{-3}$ at the Dirac point [18,19]).

A convenient way to calculate the $T = 0$ spin susceptibility for a system with SOI is via the real space retarded Green's

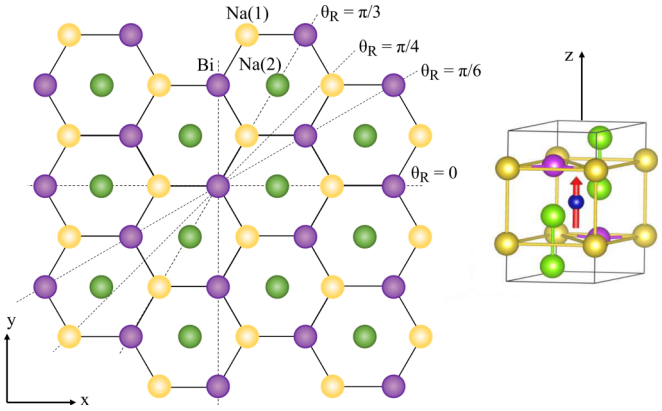

FIG. 1. Lattice structure of Na_3Bi in the xy plane (left) with dashed lines denoting different symmetry directions. Na_3Bi unit cell [24] with a magnetic impurity in its center as a possible location (right).

functions [20],

$$\chi^{\alpha,\beta}_{\mu,\mu'}(\mathbf{R}) = -\frac{1}{\pi}\mathrm{Im}\ \mathrm{Tr}\int_{-\infty}^{\omega_F}\sigma_\mu G^{\alpha,\beta}(\mathbf{R},\omega^+) \times \sigma_{\mu'} G^{\beta,\alpha}(-\mathbf{R},\omega^+)d\omega, \tag{3}$$

where $\omega^+ = \omega + i0^+$, ω_F is the Fermi energy, and the trace is over spin components. α and β denote sets of additional degrees of freedom (other than spin) that characterize the host.

Figure 1 shows the hexagonal Na_3Bi lattice structure in the xy plane and its unit cell. Following the low-energy model introduced in Ref. [21] for Na_3Bi, and applicable to Cd_3As_2 with appropriate parameters, the Hamiltonian up to second order in momentum is

$$H = \epsilon_0(\boldsymbol{k})\tau_0\sigma_0 + M(\boldsymbol{k})\tau_z\sigma_0 + A(k_x\tau_x\sigma_z - k_y\tau_y\sigma_0), \tag{4}$$

where $\epsilon_0(\boldsymbol{k}) = C_0 + C_1k_z^2 + C_2(k_x^2+k_y^2)$, $M(\boldsymbol{k}) = M_0 - M_1k_z^2 - M_2(k_x^2+k_y^2)$, and C_i, M_i, A are material dependent parameters [25]. In the case of Na_3Bi, the Hamiltonian is expressed in the basis of relevant orbitals around the linear band crossings: $(|S,\frac{1}{2}\rangle,|P,\frac{3}{2}\rangle,|S,-\frac{1}{2}\rangle,|P,-\frac{3}{2}\rangle)$, where S and P stand for bonding and antibonding orbitals between two Na-3s and Bi-6p atoms related by inversion symmetry [21]. The second quantum number in the kets indicates the z projection of the total angular momentum, upon consideration of the atomic SOI. Notice that the most relevant p-like states near the Dirac points correspond to $j=\frac{3}{2}$ and $m_j=\pm\frac{3}{2}$, where $j(j+1)$ and m_j are eigenvalues of total atomic angular momentum operators $\hat{J}^2$ and $\hat{J}_z$, respectively. The Pauli matrices τ and σ act in the $S-P$ (orbital) and total angular momentum spaces, respectively. There are two Dirac points at $\boldsymbol{K}^{\pm1} = (0,0,\pm\sqrt{M_0/M_1})$, protected by the crystalline symmetry. One can expand the Hamiltonian around these two points to get an effective low-energy model. In dimensionless form

$$H(\boldsymbol{\kappa}) = \lambda q_z\nu_z\tau_z\sigma_0 + \nu_0(k_x\tau_x\sigma_z - k_y\tau_y\sigma_0), \tag{5}$$

where $\boldsymbol{\kappa} \equiv (k_x,k_y,q_z)$, the energy is expressed in terms of $A/a = 0.451$ eV for Na_3Bi; in what follows, all the energies will be expressed in this scale. k_x,k_y are in units of the inverse lattice spacing $1/a$ ($a \simeq 5.45$ Å); q_z is the momentum in the z direction, measured from the Dirac points and in units of $1/c$ ($c \simeq 9.65$ Å). The factor $\lambda \simeq 0.25$ characterizes the Fermi velocity anisotropy in the z direction [1] ($\lambda \simeq 0.25$ for Cd_3As_2 as well [3]). The Pauli matrices ν operate in the valley degree of freedom.

From this Hamiltonian we obtain the Green's function matrix in momentum space $G(\boldsymbol{\kappa},\omega) = [\omega^+ - H(\boldsymbol{\kappa})]^{-1}$. In the present case, G is an 8×8 matrix containing orbital, angular momentum, and valley degrees of freedom. This matrix is block diagonal, and the inversion is simply calculated as an inversion of several 2×2 blocks. One gets

$$G(\boldsymbol{\kappa},\omega) = \rho(\boldsymbol{\kappa},\omega)^{-1}[\omega^+ + H(\boldsymbol{\kappa})], \tag{6}$$

where $\rho(\boldsymbol{\kappa},\omega) \equiv \omega_+^2 - k_x^2 - k_y^2 - \lambda^2q_z^2$. It is convenient to separate the Green's function in terms of the only two spin matrices in H, as [20]

$$G(\boldsymbol{\kappa}) = G_0(\boldsymbol{\kappa})\sigma_0 + G_z(\boldsymbol{\kappa})\sigma_z, \tag{7}$$

with

$$G_0(\boldsymbol{\kappa}) = \rho(\boldsymbol{\kappa},\omega)^{-1}[\omega_+ + \lambda q_z\nu_z\tau_z - k\ \sin\theta_k\nu_0\tau_y], \tag{8}$$

$$G_z(\boldsymbol{\kappa}) = \rho(\boldsymbol{\kappa},\omega)^{-1}k\cos\theta_k\nu_0\tau_x, \tag{9}$$

where we have introduced cylindrical coordinates $k = (k_x^2+k_y^2)^{\frac{1}{2}}$ and $\theta_k = \arctan(k_y/k_x)$. One can make further advances in determining the terms generated by the trace operation. As the Fourier transform does not change the spin character of the Green's function, Eq. (3) will have terms of the form $\mathrm{Tr}\,[G_0^{\alpha,\beta}(\boldsymbol{R})\sigma_\mu + G_z^{\alpha,\beta}(\boldsymbol{R})\sigma_\mu\sigma_z] \times [G_0^{\beta,\alpha}(-\boldsymbol{R})\sigma_{\mu'} + G_z^{\beta,\alpha}(-\boldsymbol{R})\sigma_{\mu'}\sigma_z]$. Then, we can write $\chi^{\alpha,\beta}_{\mu,\mu'} = -\frac{2}{\pi}\mathrm{Im}\int_{-\infty}^{\omega_F}A^{\alpha,\beta}_{\mu,\mu'}\,d\omega$, where

$$\begin{aligned} A^{\alpha,\beta}_{x,x} &= G_0^{\alpha,\beta}(\boldsymbol{R})G_0^{\beta,\alpha}(-\boldsymbol{R}) - G_z^{\alpha,\beta}(\boldsymbol{R})G_z^{\beta,\alpha}(-\boldsymbol{R}),\\ A^{\alpha,\beta}_{z,z} &= G_0^{\alpha,\beta}(\boldsymbol{R})G_0^{\beta,\alpha}(-\boldsymbol{R}) + G_z^{\alpha,\beta}(\boldsymbol{R})G_z^{\beta,\alpha}(-\boldsymbol{R}),\\ A^{\alpha,\beta}_{x,y} &= iG_0^{\alpha,\beta}(\boldsymbol{R})G_z^{\beta,\alpha}(-\boldsymbol{R}) - iG_z^{\alpha,\beta}(\boldsymbol{R})G_0^{\beta,\alpha}(-\boldsymbol{R}), \end{aligned} \tag{10}$$

with $A_{y,y} = A_{x,x}$, $A_{y,x} = -A_{x,y}$, and the remaining cross terms vanish. Using these expressions in Eq. (2), one gets in-plane XX (x,x), Ising (z,z), and DM (x,y) components

$$\begin{aligned} H_{RKKY} = J^2\big[&\chi_{x,x}\left(S_1^xS_2^x + S_1^yS_2^y\right) + \chi_{z,z}S_1^zS_2^z\\ &+ \chi_{x,y}(\boldsymbol{S}_1\times\boldsymbol{S}_2)_z\big], \end{aligned} \tag{11}$$

as expected when SOI is present [20,26–31]. The appearance of each component depends on the coupling of each impurity to the different orbital and valley degrees of freedom. There is no reason to couple inequivalently to each valley, and the susceptibility contains Green's functions which are the sum of each valley component: $G(\boldsymbol{R}) = \sum_\nu G^\nu(\boldsymbol{R})$. The products of Green's functions will generate intra- and intervalley terms in the susceptibility due to the scattering of the conduction electrons with the localized impurities.

From the Hamiltonian matrix in momentum space, one can see that S and P orbitals are connected by the propagators due to the effective SOI. In particular, we see that $G_z(\boldsymbol{\kappa})$ contains only τ_x, so the propagator does not connect S and P orbitals

to themselves: $G_z^{\nu,S,S} = G_z^{\nu,P,P} = 0$. This implies that the in-plane and Ising terms in Eq. (11) are equal and that the DM term vanishes. Therefore, if both impurities are coupled only to either S or P orbitals, the RKKY interaction will be completely isotropic (Heisenberg).

The appearance of anisotropic interactions between impurities requires one of them to be connected to an S orbital and the other to a P orbital. This does not require each impurity to be coupled to only one type of orbital. In fact, a probable impurity position would be in the middle of the tetragonal unit cell of the material (see Fig. 1), which would (locally) preserve the inversion symmetry. For impurities located at this high-symmetry point, it is expected that they would connect to both S and P orbitals, so that the effective interaction in (11) will have all three terms. Although the analysis of all possible locations and orbital configurations of the local magnetic moments is beyond the scope of this paper, in the following we analyze the possible diagonal and nondiagonal orbital components for the different interactions. Analysis of the exchange interactions along different lattice directions would be seen to depend crucially on orbital hybridization.

III. RESULTS

A. Diagonal orbital components

When both impurities connect to the same type of orbital, we have that $G_0^{\nu=1,S,S}(\boldsymbol{\kappa}) = G_0^{\nu=-1,P,P}(\boldsymbol{\kappa}) = \rho(\boldsymbol{\kappa},\omega)^{-1}(\omega_+ + \lambda q_z)$, and $G_0^{\nu=-1,S,S}(\boldsymbol{\kappa}) = G_0^{\nu=1,P,P}(\boldsymbol{\kappa}) = \rho(\boldsymbol{\kappa},\omega)^{-1}(\omega_+ - \lambda q_z)$. The real space version, after integration on θ_k and k [in the $(0,\infty)$ range, valid for large impurity separations], can be written as

$$G_0^{\nu,S,S}(\mathbf{R}) = -\frac{e^{i\nu K_z R_z}}{(2\pi)^2}\int_{-\infty}^{\infty} e^{iq_z R_z}(\omega_+ + \nu\lambda q_z) \times K_0\big(R\sqrt{\lambda^2 q_z^2 - \omega_+^2}\big)dq_z, \tag{12}$$

where $\mathbf{R}$ is in cylindrical coordinates, R is the radial coordinate in the xy plane, and K_0 is the Bessel function. k_z has been replaced by $\pm K_z + q_z$. The analytic continuation $\omega^+ \to \omega$ and the branch cut in the square root allow one to write

$$G_0^{\nu,S,S}(\mathbf{R}) = -\frac{e^{i\nu K_z R_z}}{(2\pi)^2}(I_0 - i\,\mathrm{sgn}(\omega) I_1), \tag{13}$$

where

$$I_0 = \left(\int_{-\infty}^{-\frac{|\omega|}{\lambda}} + \int_{\frac{|\omega|}{\lambda}}^{\infty}\right) e^{iq_z R_z}(\omega + \nu\lambda q_z) K_0(u) dq_z,$$
$$I_1 = \int_{-\frac{|\omega|}{\lambda}}^{\frac{|\omega|}{\lambda}} e^{iq_z R_z}(\omega + \nu\lambda q_z) K_0(-i\,\mathrm{sgn}(\omega) v) dq_z, \tag{14}$$

with $u = R\sqrt{\lambda^2 q_z^2 - \omega^2}$ and $v = R\sqrt{\omega^2 - \lambda^2 q_z^2}$. Lacking analytical solutions, we proceed with the case $R \gg R_z$, which allows one to obtain asymptotic expressions. Considering the case where the Fermi energy lies below the Dirac points, $\omega < 0$, and adding the contributions of the two valleys, one gets (Appendix A)

$$G_0^{S,S}(\mathbf{R},\omega) \simeq -\frac{1}{\pi^2\lambda R^2}\left(e^{\frac{i3\pi}{4}}\cos\left(K_z R_z - \frac{|\omega| R_z}{\lambda}\right) + i\frac{\pi\omega R}{2}\exp\left(iR\omega\left[1 + \frac{R_z^2}{2\lambda^2 R^2}\right]\right) \times \left[\cos(K_z R_z) + i\frac{R_z}{\lambda R}\sin(K_z R_z)\right]\right), \tag{15}$$

with the same expression for $G_0^{P,P}(\mathbf{R},\omega)$. We can now calculate the susceptibility, by integrating over ω. The integration generates many terms, with the most relevant in the R asymptotic limit given by

$$\chi_{x,x}^{S,S}(\mathbf{R},\omega_F) = \chi_{z,z}^{P,P}(\mathbf{R},\omega_F) \simeq -\frac{\omega_F^2}{4\pi^3\lambda^2 R^3}\cos^2(K_z R_z) \times \cos\left(2R\left[1 + \frac{R_z^2}{2\lambda^2 R^2}\right]\omega_F\right). \tag{16}$$

Notice there is no angular dependence. These effective in-plane spin-spin interactions decay as $1/R^3$, while there is no decay for separations in the z direction; they only oscillate with R_z ($\ll R$). There are, however, important corrections due to the dispersion anisotropy. The form of the spatial term inside the second cosine comes from a second order expansion of an effective distance given by $\hat{R} \equiv \sqrt{R^2 + \lambda^2 R_z^2} \simeq R[1 + \frac{R_z^2}{2\lambda^2 R^2}]$. For $\lambda = 1$, which corresponds to a completely isotropic Fermi velocity, we recover the expected isotropic distance dependence in 3D. Another important effect of the anisotropy is to modulate the amplitude of the interaction. It decreases for $\lambda > 1$, with respect to the isotropic case. For materials with $\lambda < 1$, such as Na_3Bi and Cd_3As_2, the interaction is significantly enhanced (Fig. 2). Notice that the interaction decays quadratically in energy towards the Dirac point. The interesting oscillatory (and always positive) term that comes from intervalley scattering modulates the usual oscillatory RKKY term. When $K_z R_z$ is an odd multiple of $\frac{\pi}{2}$, the interaction vanishes for any value of R or band

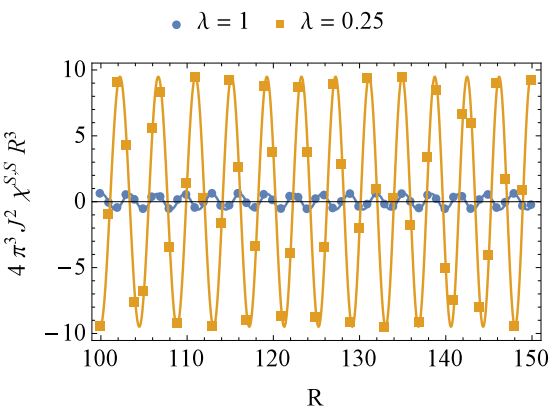

FIG. 2. Effective impurity interaction as a function of their separation R in the xy plane. The anisotropy in the Fermi velocity, characterized by $\lambda = 0.25$, has a big impact on the strength of the interaction with respect to the isotropic case ($\lambda = 1$). It also introduces a correction in the period of the oscillation.

filling. In Na_3Bi, where $K_z \simeq 0.82 \times \frac{1}{c}$, this will happen for $R_z \simeq 3.83(n - \frac{1}{2})c$, where n is an integer. Exactly at the Dirac nodes, $\omega_F = 0$, $\chi^{S,S}$ in Eq. (16) vanishes at the third order in the asymptotic expansion in R. At the next order in the expansion, one gets no oscillation with the in-plane distance R, and $\sim R^{-4}$ decay.

B. Off-diagonal orbital components

Now we consider the case in which one impurity is connected to an S orbital and the second one to a P orbital. The Green's functions have the following properties: $G_0^{\nu,S,P}(\boldsymbol{\kappa},\omega) = -G_0^{\nu,P,S}(\boldsymbol{\kappa},\omega) = i\rho(\boldsymbol{\kappa},\omega)^{-1}k\,\sin\theta_k$. Proceeding in a similar way as in the diagonal case, one gets (Appendix B)

$$G_0^{S,P}(\mathbf{R},\omega) \simeq \frac{\sin(\theta_R)}{2\pi^2}\cos(K_z R_z)\, f(R,R_z,\omega), \tag{17}$$

$$G_z^{S,P}(\mathbf{R},\omega) \simeq \frac{i\,\cos(\theta_R)}{2\pi^2}\cos(K_z R_z)\, f(R,R_z,\omega), \tag{18}$$

where

$$f(R,R_z,\omega) = -\frac{1}{\lambda R^2}\left[\frac{4}{R\omega}\left(1+\frac{i}{\pi}\right)\cos\left(\frac{|R_z|\omega}{\lambda}\right) + i\pi\omega\left(\exp\left(iR\omega\left[1+\frac{R_z^2}{2\lambda^2R^2}\right]\right)\times\left[R\omega\left(\frac{R_z^2}{\lambda^2R^2}-1\right)+i\left(\frac{R_z^4\omega^2}{8\lambda^4R^2}-1\right)\right]\right)\right], \tag{19}$$

for $\omega < 0$. After integrating over ω, and retaining the most relevant asymptotic terms in R, we get (Appendix B)

$$\begin{aligned}\chi_{x,x}^{S,P}(\mathbf{R},\omega_F) &\simeq -\chi_{x,x}^{S,S}(\mathbf{R},\omega_F)\cos(2\theta_R),\\ \chi_{z,z}^{S,P}(\mathbf{R},\omega_F) &\simeq \chi_{x,x}^{S,S}(\mathbf{R},\omega_F),\\ \chi_{x,y}^{S,P}(\mathbf{R},\omega_F) &\simeq -\chi_{x,x}^{S,S}(\mathbf{R},\omega_F)\sin(2\theta_R),\end{aligned} \tag{20}$$

where $\chi_{x,x}^{S,S}$ is given by Eq. (16). Unlike the case of the diagonal orbital components, now there is a strong angular dependence in the in-plane interaction, while the Ising component is angle independent (see Fig. 1 for a schematic of high symmetry directions). We can see that along the x direction, $\theta_R = 0$, the DM term vanishes and one ends up with an interaction where the in-plane and Ising terms are out of phase (opposite signs), but with the same magnitude. When $\theta_R = \pi/4$, the in-plane Heisenberg term vanishes so only Ising and DM terms survive, with equal strength and in phase. For separations along the y axis, $\theta_R = \frac{\pi}{2}$, the DM term vanishes, which produces a completely isotropic Heisenberg interaction, as in the case without orbital mixing. There are two other high symmetry directions in the lattice. One corresponds to angles $\theta_R = \pm\frac{\pi}{6}$ (see Fig. 1). These angles give prefactors for the different terms: $\frac{1}{2}$ for XX and $\pm\frac{\sqrt{3}}{2}$ for DM. This implies that the Ising component dominates over the other two in this direction, its magnitude twice XX, and out of phase with each other. At the same time, the DM term is $\sqrt{3}$ times bigger than the isotropic in-plane (but smaller than Ising), and its sign depends on the specific direction. For $\theta_R = \pm\frac{2\pi}{3}$, the prefactors are $-\frac{1}{2}$ and $\mp\frac{\sqrt{3}}{2}$ for XX and DM, respectively, which makes it similar to the former but with different relative phases. Other angles (lattice directions) produce interactions that mix all three components, giving a tendency to complex spiral ordering of spins embedded in this lattice. Exactly at the Dirac point, we find that the decay is even faster than for the diagonal case, $\chi^{S,P} \sim R^{-5}$, and again it does not oscillate.

A likely location for impurities is at the center of the unit cell (Fig. 1). There, it preserves inversion symmetry locally. It is probable that each impurity will hybridize to both S and P orbitals, in which case the effective interaction will have contributions from both diagonal and off-diagonal components. It is worth mentioning that a DM term is expected to appear in systems with SOI and absence of inversion symmetry. Both conditions are satisfied in the presence of Rashba SOI [20,26–28]. Materials with intrinsic SOI and absence of an underlying crystalline inversion symmetry, such as monolayer transition metal dichalcogenides [30,31], are another example. In the present case, the multicomponent spinor nature of the states allows nonzero DM terms even with inversion symmetry, provided that each impurity hybridizes unequally to each orbital.

In the simple case in which the hybridization to each orbital is of the same magnitude, one can add all the components to obtain the final effective interaction. Given that $\chi_{x,y}^{P,S} = -\chi_{x,y}^{S,P}$, the DM term will vanish, and $\chi_{x,x} = 4\sin^2(\theta_R)\chi_{x,x}^{S,S}$, $\chi_{z,z} = 4\chi_{x,x}^{S,S}$. In this case we recover an isotropic interaction for $\theta_R = \frac{\pi}{2}$, and for $\theta_R = 0,\pi$ the interaction is only along the z direction.

IV. CONCLUSIONS

We have obtained asymptotic expressions for the RKKY interaction in 3D Dirac semimetals. In the limit in which $R \gg R_z$, the indirect coupling decays as R^{-3}, where R is the impurity separation in the xy plane. There are three important factors that come into play for the resultant interaction. First, the Fermi velocity anisotropy modifies the period of the oscillation as a function of the impurity separation, and also its magnitude. Second, the position of the Dirac points in the Brillouin zone, given by K_z, results in a second modulation along the z direction, with a period that depends on the K_z value. Lastly, the orbitals to which the impurities hybridize have impact on the angular dependence of the interaction in the xy plane. When both impurities couple to the same type of orbital (S or P), the interaction is angular independent. When impurities hybridize to a different orbital, there is a strong modulation with the orientation in the lattice. The different components of the interaction survive depending on the directions along the crystal, resulting in complex equilibrium configurations for an impurity ensemble. These results can be tested by NMR and μSR experiments.

Note added. Recently, we became aware of two papers [32,33] which analyze the RKKY interaction in Weyl semimetals. Our results are similar to the ones in Ref. [32] for the distance dependence of the interaction and the effect of the Fermi velocity anisotropy.

ACKNOWLEDGMENTS

This work was supported by NSF Grant No. DMR-1508325.

APPENDIX A: CALCULATION DETAILS FOR DIAGONAL ORBITAL COMPONENTS

We start by considering the case in which each impurity is hybridized to the same type of orbital, either S or P. In this case we have that $G_0^{\nu=1,S,S}(\mathbf{R}) = G_0^{\nu=-1,P,P}(\mathbf{R}) = \rho^{-1}(\omega_+ + \lambda q_z)$, and $G_0^{\nu=-1,S,S}(\mathbf{R}) = G_0^{\nu=1,P,P}(\mathbf{R}) = \rho^{-1}(\omega_+ - \lambda q_z)$. Then,

$$G_0^{\nu,S,S}(\boldsymbol{R},\omega) = \frac{1}{(2\pi)^3}\int G_0^{\nu,S,S}(\boldsymbol{\kappa},\omega)e^{i\mathbf{k}\cdot\mathbf{R}}d\mathbf{k} = -\frac{e^{i\nu K_z R_z}}{(2\pi)^2}\int_{-\infty}^{\infty} e^{iq_z R_z}(\omega_+ + \nu\lambda q_z)K_0\big(R\sqrt{\lambda^2 q_z^2 - \omega_+^2}\big)dq_z, \tag{A1}$$

with $\mathbf{R}$ expressed in cylindrical coordinates, where R is the radial coordinate in the xy plane, and K_0 is the modified Bessel function of the second kind. In Eq. (A1) we have already integrated over the angle θ_k, and also over k in the $(0,\infty)$ range, which is a valid approximation for large impurity separation. k_z has been replaced by $\pm K_z + q_z$ as well, and we are left with the integration over q_z. Using the fact that

$$\sqrt{\lambda^2 q_z^2 - \omega_+^2} = \begin{cases} \sqrt{\lambda^2 q_z^2 - \omega^2}, & |\omega| \leqslant \lambda q_z, \\ -i\ \mathrm{sgn}(\omega)\sqrt{\omega^2 - \lambda^2 q_z^2}, & |\omega| > \lambda q_z. \end{cases} \tag{A2}$$

we get that

$$G_0^{\nu,S,S}(\mathbf{R},\omega) = -\frac{e^{i\nu K_z R_z}}{(2\pi)^2}[I_{0a} - i\ \mathrm{sgn}(\omega) I_{0b}], \tag{A3}$$

where

$$I_{0a} = \left(\int_{-\infty}^{-\frac{|\omega|}{\lambda}} + \int_{\frac{|\omega|}{\lambda}}^{\infty}\right) e^{iq_z R_z}(\omega + \nu\lambda q_z)K_0\big(R\sqrt{\lambda^2 q_z^2 - \omega^2}\big)dq_z \tag{A4}$$

and

$$I_{0b} = \int_{-\frac{|\omega|}{\lambda}}^{\frac{|\omega|}{\lambda}} e^{iq_z R_z}(\omega + \nu\lambda q_z)K_0\big(-i\ \mathrm{sgn}(\omega)R\sqrt{\omega^2 - \lambda^2 q_z^2}\big)dq_z. \tag{A5}$$

Using the identities

$$K_0(ix) = i\frac{\pi}{2}H_0^{(1)}(x) = i\frac{\pi}{2}[J_0(x) + iY_0(x)] \quad (x \in \mathbb{R}), \tag{A6}$$

we get that

$$K_0\big(-i\ \mathrm{sgn}(\omega)R\sqrt{\omega^2 - \lambda^2 q_z^2}\big) = -\frac{\pi}{2}\big[Y_0\big(R\sqrt{\omega^2 - \lambda^2 q_z^2}\big) - i\ \mathrm{sgn}(\omega)J_0\big(R\sqrt{\omega^2 - \lambda^2 q_z^2}\big)\big], \tag{A7}$$

so

$$I_{0b} = -\frac{\pi}{2}\int_{-\frac{|\omega|}{\lambda}}^{\frac{|\omega|}{\lambda}} e^{iq_z R_z}(\omega + \nu\lambda q_z)\big[Y_0\big(R\sqrt{\omega^2 - \lambda^2 q_z^2}\big) - i\ \mathrm{sgn}(\omega)J_0\big(R\sqrt{\omega^2 - \lambda^2 q_z^2}\big)\big]dq_z, \tag{A8}$$

and using the parity properties of the integrand under $q_z \to -q_z$, we can write

$$I_{0a} = 2\omega\int_{\frac{|\omega|}{\lambda}}^{\infty} \cos(q_z R_z)K_0\big(R\sqrt{\lambda^2 q_z^2 - \omega^2}\big)dq_z + 2i\nu\lambda\int_{\frac{|\omega|}{\lambda}}^{\infty} q_z \sin(q_z R_z)K_0\big(R\sqrt{\lambda^2 q_z^2 - \omega^2}\big)dq_z \tag{A9}$$

and

$$I_{0b} = -\pi(I_{0b,1} + I_{0b,2} + I_{0b,3} + I_{0b,4}), \tag{A10}$$

where

$$\begin{aligned} I_{0b,1} &= \omega\int_0^{\frac{|\omega|}{\lambda}} \cos(q_z R_z)Y_0\big(R\sqrt{\omega^2 - \lambda^2 q_z^2}\big)dq_z, \\ I_{0b,2} &= -i|\omega|\int_0^{\frac{|\omega|}{\lambda}} \cos(q_z R_z)J_0\big(R\sqrt{\omega^2 - \lambda^2 q_z^2}\big)dq_z, \\ I_{0b,3} &= i\nu\lambda\int_0^{\frac{|\omega|}{\lambda}} q_z \sin(q_z R_z)Y_0\big(R\sqrt{\omega^2 - \lambda^2 q_z^2}\big)dq_z, \\ I_{0b,4} &= \nu\lambda\ \mathrm{sgn}(\omega)\int_0^{\frac{|\omega|}{\lambda}} q_z \sin(q_z R_z)J_0\big(R\sqrt{\omega^2 - \lambda^2 q_z^2}\big)dq_z. \end{aligned} \tag{A11}$$

These integrals cannot be solved in a closed form. Substituting $u = R\sqrt{\lambda^2 q_z^2 - \omega^2}$ in I_{0a}, $v = R\sqrt{\omega^2 - \lambda^2 q_z^2}$ in I_{0b}, and defining $r = \frac{|R_z|}{\lambda R}$, $\alpha = R|\omega|$, we get

$$\begin{aligned} I_{0a,1} &= \frac{2\omega}{\lambda R}\int_0^\infty \frac{u}{\sqrt{\alpha^2+u^2}}\cos(r\sqrt{\alpha^2+u^2})K_0(u)du, \\ I_{0a,2} &= i\frac{2\nu\ \mathrm{sgn}(R_z)}{\lambda R^2}\int_0^\infty u\ \sin(r\sqrt{\alpha^2+u^2})K_0(u)du, \end{aligned} \tag{A12}$$

and

$$\begin{aligned} I_{0b,1} &= \frac{\omega}{\lambda R}\int_0^\alpha \frac{v}{\sqrt{\alpha^2-v^2}}\cos(r\sqrt{\alpha^2-v^2})Y_0(v)dv, \\ I_{0b,2} &= -i\frac{|\omega|}{\lambda R}\int_0^\alpha \frac{v}{\sqrt{\alpha^2-v^2}}\cos(r\sqrt{\alpha^2-v^2})J_0(v)dv, \\ I_{0b,3} &= i\frac{\nu\ \mathrm{sgn}(R_z)}{\lambda R^2}\int_0^\alpha v\ \sin(r\sqrt{\alpha^2-v^2})Y_0(v)dv, \\ I_{0b,4} &= \frac{\nu\ \mathrm{sgn}(\omega R_z)}{\lambda R^2}\int_0^\alpha v\ \sin(r\sqrt{\alpha^2-v^2})J_0(v)dv. \end{aligned} \tag{A13}$$

We tackle the integrals in the limit $r \ll 1$, expanding the sines and cosines around $r = 0$ as

$$\begin{aligned} \sin(r\sqrt{\alpha^2\pm u^2}) &= \sum_{n=0}^\infty \frac{(-1)^n}{(2n+1)!}(r\sqrt{\alpha^2\pm u^2})^{2n+1}, \\ \cos(r\sqrt{\alpha^2\pm u^2}) &= \sum_{n=0}^\infty \frac{(-1)^n}{(2n)!}(r\sqrt{\alpha^2\pm u^2})^{2n}. \end{aligned} \tag{A14}$$

Then we have that

$$\begin{aligned} \int_0^\infty u(\sqrt{\alpha^2+u^2})^{2n-1}K_0(u)du &= \frac{2^{2n-1}}{\Gamma\left(\frac{1}{2}-n\right)}G^{3,1}_{1,3}\left(\begin{matrix} n+\frac{1}{2} \\ 0,n+\frac{1}{2},n+\frac{1}{2}\end{matrix}\ \middle|\ \frac{\alpha^2}{4}\right), \\ \int_0^\alpha v(\sqrt{\alpha^2+v^2})^{2n-1}Y_0(v) &= 4^n\Gamma\left(n+\frac{1}{2}\right)G^{2,1}_{2,4}\left(\begin{matrix} n+\frac{1}{2},n \\ n+\frac{1}{2},n+\frac{1}{2},0,n\end{matrix}\ \middle|\ \frac{\alpha^2}{4}\right), \\ \int_0^\alpha v(\sqrt{\alpha^2-v^2})^{2n-1}J_0(v)dv &= 2^{n-\frac{1}{2}}\Gamma\left(n+\frac{1}{2}\right)J_{n+\frac{1}{2}}(\alpha), \end{aligned} \tag{A15}$$

where $G^{m,n}_{p,q}$ is the Meijer function. The summations cannot be done analytically as they are, but we can use asymptotic expansions in α

$$\begin{aligned} G^{3,1}_{1,3}\left(\begin{matrix} n+\frac{1}{2} \\ 0,n+\frac{1}{2},n+\frac{1}{2}\end{matrix}\ \middle|\ \frac{\alpha^2}{4}\right) &\simeq 4^{\frac{1}{2}-n}\Gamma\left(\frac{1}{2}-n\right)\alpha^{2n-1}, \\ G^{2,1}_{2,4}\left(\begin{matrix} n+\frac{1}{2},n \\ n+\frac{1}{2},n+\frac{1}{2},0,n\end{matrix}\ \middle|\ \frac{\alpha^2}{4}\right) &\simeq \frac{4^{-n}\alpha^n}{\pi}\left(\frac{2\alpha^{n-1}}{\Gamma\left(n+\frac{1}{2}\right)}-\sqrt{\pi}2^n\cos\left(\alpha-\frac{\pi n}{2}\right)\right), \\ J_{n+\frac{1}{2}}(\alpha) &\simeq \sqrt{\frac{2}{\pi\alpha}}\sin\left(\alpha-\frac{\pi n}{2}\right). \end{aligned} \tag{A16}$$

Now the summation can be performed, and we get

$$\begin{aligned}
\Sigma_{0a,1}(\alpha,r) &= \sum_{n=0}^{\infty} \frac{(-1)^n \alpha^{2n-1} r^{2n}}{(2n)!} = \frac{\cos(r\alpha)}{\alpha},\\
\Sigma_{0a,2}(\alpha,r) &= \sum_{n=0}^{\infty} \frac{(-1)^n \alpha^{2n+1} r^{2n+1}}{(2n+1)!} = \sin(r\alpha),\\
\Sigma_{0b,1}(\alpha,r) &= \sum_{n=0}^{\infty} \frac{(-1)^n\ r^{2n}}{(2n)!}\left[\frac{2\alpha^{2n-1}}{\pi} - \frac{2^n\alpha^n}{\sqrt{\pi}}\Gamma\left(n+\frac{1}{2}\right)\cos\left(\alpha-\frac{n\pi}{2}\right)\right] = \frac{2}{\pi\alpha}\cos(r\alpha) - \cos\left(\alpha\left[1+\frac{r^2}{2}\right]\right),\\
\Sigma_{0b,2}(\alpha,r) &= -\sqrt{\frac{2}{\pi\alpha}}\sum_{n=0}^{\infty} \frac{(-1)^n r^{2n}}{(2n)!} 2^{n-\frac{1}{2}}\alpha^{n+\frac{1}{2}}\Gamma\left(n+\frac{1}{2}\right)\sin\left(\alpha-\frac{\pi n}{2}\right) = \sin\left(\alpha\left[1+\frac{r^2}{2}\right]\right),\\
\Sigma_{0b,3}(\alpha,r) &= \sum_{n=0}^{\infty} \frac{(-1)^n r^{2n+1}}{(2n+1)!}\frac{\alpha^{n+1}}{\pi 2^{2n+1}}\left(\frac{\alpha^n}{\Gamma\left(n+\frac{3}{2}\right)} - \sqrt{\pi}2^n\sin\left(\alpha-\frac{\pi n}{2}\right)\right) = \frac{2}{\pi}\sin(r\alpha) - r\alpha\ \sin\left(\alpha\left[1+\frac{r^2}{2}\right]\right),\\
\Sigma_{0b,4}(\alpha,r) &= -\sqrt{\frac{2}{\pi\alpha}}\sum_{n=0}^{\infty} \frac{(-1)^n r^{2n+1}}{(2n+1)!} 2^{n+\frac{1}{2}}\alpha^{n+\frac{3}{2}}\Gamma\left(n+\frac{3}{2}\right)\cos\left(\alpha-\frac{\pi n}{2}\right) = -r\alpha\ \cos\left(\alpha\left[1+\frac{r^2}{2}\right]\right).
\end{aligned} \tag{A17}$$

Then

$$\begin{aligned}
I_{0a,1} &\simeq \frac{2\omega}{\lambda r}\Sigma_1(\alpha,r) = \frac{2\omega\ \cos(r\alpha)}{\lambda R\alpha} = \frac{2\ \mathrm{sgn}(\omega)}{\lambda R^2}\cos\left(\frac{|R_z\omega|}{\lambda}\right),\\
I_{0a,2} &\simeq i\frac{2\nu\ \mathrm{sgn}(R_z)}{\lambda R^2}\Sigma_2(\alpha,r) = i\frac{2\nu\ \mathrm{sgn}(R_z)}{\lambda R^2}\sin(r\alpha) = i\frac{2\nu\ \mathrm{sgn}(R_z)}{\lambda R^2}\sin\left(\frac{|R_z\omega|}{\lambda}\right),
\end{aligned} \tag{A18}$$

which results in

$$I_{0a}(R,R_z,\omega,\nu) \simeq \frac{2}{\lambda R^2}\,\mathrm{sgn}(\omega)\exp\left(i\nu\frac{\omega R_z}{\lambda}\right), \quad |Rz| \ll \lambda R. \tag{A19}$$

On the other hand,

$$\begin{aligned}
I_{0b,1} &\simeq \frac{\omega}{\lambda R}\Sigma_{0b,1}(\alpha,r) = \frac{\omega}{\lambda R}\left[\frac{2}{\pi R|\omega|}\cos\left(\frac{|\omega R_z|}{\lambda}\right) - \cos\left(R|\omega|\left[1+\frac{R_z^2}{2\lambda^2R^2}\right]\right)\right],\\
I_{0b,2} &\simeq -i\frac{|\omega|}{\lambda R}\Sigma_{0b,2}(\alpha,r) = -i\frac{|\omega|}{\lambda R}\sin\left(R|\omega|\left[1+\frac{R_z^2}{2\lambda^2R^2}\right]\right),\\
I_{0b,3} &\simeq i\frac{\nu\ \mathrm{sgn}(R_z)}{\lambda R^2}\Sigma_{0b,3}(\alpha,r) = i\frac{\nu\ \mathrm{sgn}(R_z)}{\lambda R^2}\left[\frac{2}{\pi}\sin\left(\frac{|\omega R_z|}{\lambda}\right) - \frac{|\omega R_z|}{\lambda}\sin\left(R|\omega|\left[1+\frac{R_z^2}{2\lambda^2R^2}\right]\right)\right],\\
I_{0b,4} &\simeq \frac{\nu\ \mathrm{sgn}(\omega R_z)}{\lambda R^2}\Sigma_{0b,4}(\alpha,r) = -\frac{\nu R_z\omega}{\lambda^2R^2}\cos\left(R|\omega|\left[1+\frac{R_z^2}{2\lambda^2R^2}\right]\right).
\end{aligned} \tag{A20}$$

After some algebra, one finds that

$$I_{0b}(R,R_z,\omega,\nu) = -\frac{\pi}{\lambda R}\,\mathrm{sgn}(\omega)\left[\frac{2}{\pi R}\exp\left(i\nu\frac{\omega R_z}{\lambda}\right) - |\omega|\left(1+\nu\frac{R_z}{\lambda R}\right)\exp\left(iR\omega\left[1+\frac{R_z^2}{2\lambda^2R^2}\right]\right)\right], \quad |Rz| \ll \lambda R. \tag{A21}$$

For $\omega < 0$, this gives rise to the Green's function appearing in Eq. (15).

APPENDIX B: OFF-DIAGONAL ORBITAL COMPONENTS

When one of the impurities hybridizes with an S orbital and the other one with a P orbital, we have that $G_0^{\nu,S,P}(\kappa,\omega) = -G_0^{\nu,P,S}(\kappa,\omega) = i\rho^{-1}k\ \sin\theta_k$. The Fourier transform gives

$$G_0^{\nu,S,P}(\mathbf{R},\omega) = \frac{i}{(2\pi)^3}\int_{-\infty}^{\infty} dk_z e^{ik_zR_z}\int_0^{\infty} dk\frac{k^2}{\rho}\int_0^{2\pi} d\theta_k \sin\theta_k e^{ikR\ \cos(\theta_k-\theta_R)}. \tag{B1}$$

Integrating over θ_k, we get

$$G_0^{\nu,S,P}(\mathbf{R},\omega) = -\frac{\sin(\theta_R)}{4\pi^2}\int_{-\infty}^{\infty} dk_z e^{ik_zR_z}\int_0^{\infty} dk\frac{k^2}{\rho}J_1(kR). \tag{B2}$$

Integrating over k and replacing k_z by $K_z^\tau + q_z$, we get

$$G_0^{\nu,S,P}(\mathbf{R},\omega) = \frac{\sin(\theta_R)}{4\pi^2} e^{iK_z^\tau R_z} \int_{-\infty}^{\infty} dq_z e^{iq_z R_z} \sqrt{\lambda^2 q_z^2 - \omega_+^2}\, K_1\big(R\sqrt{\lambda^2 q_z^2 - \omega_+^2}\big), \tag{B3}$$

which can be written as

$$G_0^{\nu,S,P}(\mathbf{R},\omega) = \frac{\sin(\theta_R)}{4\pi^2} e^{iK_z^\nu R_z}[I_2 - i\ \mathrm{sgn}(\omega) I_3], \tag{B4}$$

where

$$I_2 = \left(\int_{-\infty}^{-\frac{|\omega|}{\lambda}} + \int_{\frac{|\omega|}{\lambda}}^{\infty}\right) e^{iq_z R_z} \sqrt{\lambda^2 q_z^2 - \omega^2}\, K_1\big(R\sqrt{\lambda^2 q_z^2 - \omega^2}\big) dq_z \tag{B5}$$

and

$$I_3 = \int_{-\frac{|\omega|}{\lambda}}^{\frac{|\omega|}{\lambda}} e^{iq_z R_z} \sqrt{\omega^2 - \lambda^2 q_z^2}\, K_1\big(-iR\ \mathrm{sgn}(\omega)\sqrt{\omega^2 - \lambda^2 q_z^2}\big) dq_z. \tag{B6}$$

Similarly,

$$G_z^{\nu,S,P}(\mathbf{R},\omega) = \frac{i\ \cos(\theta_R)}{4\pi^2} e^{iK_z^\nu R_z}[I_2 - i\ \mathrm{sgn}(\omega) I_3], \tag{B7}$$

with $G_z^{\nu,P,S}(\mathbf{R},\omega) = G_z^{\nu,S,P}(\mathbf{R},\omega)$. Changing variables as in the previous case, we get

$$I_2 = \frac{2}{\lambda R^2} \int_0^{\infty} \frac{u^2 K_1(u)}{\sqrt{u^2 + R^2\omega^2}} \cos\left(\frac{R_z}{\lambda R}\sqrt{u^2 + R^2\omega^2}\right) du. \tag{B8}$$

This expression is even under $\omega \to -\omega$ and $R_z \to -R_z$, then

$$I_2 = \frac{2}{\lambda R^2} \int_0^{\infty} \frac{u^2 K_1(u)}{\sqrt{u^2 + \alpha^2}} \cos(r\sqrt{u^2 + \alpha^2}) du. \tag{B9}$$

Similarly, for I_3 we have

$$I_3 = -\frac{\pi}{\lambda R^2} \int_0^{\alpha} \frac{v^2 H_1^{(1)}[\mathrm{sgn}(\omega) v]}{\sqrt{\alpha^2 - v^2}} \cos(r\sqrt{\alpha^2 - v^2}) dv = -\frac{\pi}{\lambda R^2} \int_0^{\alpha} \frac{v^2[iY_1(v) + \mathrm{sgn}(\omega) J_1(v)]}{\sqrt{\alpha^2 - v^2}} \cos(r\sqrt{\alpha^2 - v^2}) dv, \tag{B10}$$

or

$$I_3 = -\frac{\pi}{\lambda R^2}[\mathrm{sgn}(\omega) I_{3a} + i I_{3b}], \tag{B11}$$

where

$$I_{3a} = \int_0^{\alpha} \frac{v^2 J_1(v)}{\sqrt{\alpha^2 - v^2}} \cos(r\sqrt{\alpha^2 - v^2}) dv, \tag{B12}$$

$$I_{3b} = \int_0^{\alpha} \frac{v^2 Y_1(v)}{\sqrt{\alpha^2 - v^2}} \cos(r\sqrt{\alpha^2 - v^2}) dv. \tag{B13}$$

Using the cosine series expansions, we get

$$\int_0^{\infty} u^2 K_1(u)(u^2 + \alpha^2)^{n-\frac{1}{2}} du = \frac{2^{2n-3}\alpha^3}{\Gamma\left(\frac{1}{2} - n\right)} G_{1,3}^{3,1}\left(\begin{matrix} n-1 \\ -\frac{3}{2}, n-1, n \end{matrix} \middle| \frac{\alpha^2}{4}\right), \tag{B14}$$

$$\int_0^{\alpha} v^2 J_1(v)(\alpha^2 - v^2)^{n-\frac{1}{2}} dv = 2^{n-\frac{1}{2}} \Gamma\left(n + \frac{1}{2}\right) \alpha^{n+\frac{3}{2}} J_{n+\frac{3}{2}}(\alpha), \tag{B15}$$

$$\int_0^{\alpha} v^2 Y_1(v)(\alpha^2 - v^2)^{n-\frac{1}{2}} dv = 2^{n-\frac{1}{2}} \Gamma\left(n + \frac{1}{2}\right) \alpha^{n+\frac{3}{2}} Y_{n+\frac{3}{2}}(\alpha) + \frac{4}{\pi}\alpha^{2n-1}. \tag{B16}$$

The summations cannot be performed analytically, so we expand the special functions for $\alpha \gg 1$

$$G_{1,3}^{3,1}\left(\begin{matrix} n-1 \\ -\frac{3}{2}, n-1, n \end{matrix} \middle| \frac{\alpha^2}{4}\right) \simeq 4^{2-n}\alpha^{2(n-2)} \Gamma\left(\frac{1}{2} - n\right), \tag{B17}$$

$$J_{n+\frac{3}{2}}(\alpha) \simeq -\sqrt{\frac{2}{\pi\alpha}} \cos\left(\alpha - \frac{\pi n}{2}\right) + \frac{(n+1)(n+2)}{\sqrt{2\pi}\,\alpha^{3/2}} \sin\left(\alpha - \frac{\pi n}{2}\right), \tag{B18}$$

$$Y_{n+\frac{3}{2}}(\alpha) \simeq -\sqrt{\frac{2}{\pi\alpha}}\sin\left(\alpha-\frac{\pi n}{2}\right)-\frac{(n+1)(n+2)}{\sqrt{2\pi}\,\alpha^{3/2}}\cos\left(\alpha-\frac{\pi n}{2}\right). \tag{B19}$$

Proceeding with the summations, we get

$$\Sigma_2(\alpha,r)=2\sum_{n=0}^{\infty}\frac{(-1)^n}{(2n)!}r^{2n}\alpha^{3+2(n-2)}=\frac{2\,\cos(r\alpha)}{\alpha}, \tag{B20}$$

$$\Sigma_{3a}(\alpha,r)=-\frac{1}{\sqrt{\pi}}\sum_{n=0}^{\infty}\frac{(-1)^n}{(2n)!}r^{2n}2^{n-1}\alpha^n\Gamma\left(n+\frac{1}{2}\right)\left[(n+1)(n+2)\sin\left(\frac{\pi n}{2}-\alpha\right)+2\alpha\,\cos\left(\frac{\pi n}{2}-\alpha\right)\right] \tag{B21}$$

$$=\alpha(r^2-1)\cos\left(\alpha+\frac{\alpha r^2}{2}\right)-\left(\frac{\alpha^2r^4}{8}-1\right)\sin\left(\alpha+\frac{\alpha r^2}{2}\right), \tag{B22}$$

$$\Sigma_{3b}(\alpha,r)=-\sum_{n=0}^{\infty}\frac{(-1)^n}{(2n)!}r^{2n}\left(2^{n-1}\alpha^{n+\frac{3}{2}}\Gamma\left(n+\frac{1}{2}\right)\left[\sqrt{\frac{2}{\pi\alpha}}\sin\left(\alpha-\frac{\pi n}{2}\right)+\frac{(n+1)(n+2)}{\sqrt{2\pi}\,\alpha^{3/2}}\cos\left(\alpha-\frac{\pi n}{2}\right)\right]-\frac{4}{\pi}\alpha^{2n-1}\right) \tag{B23}$$

$$=\alpha(r^2-1)\sin\left(\alpha+\frac{\alpha r^2}{2}\right)+\left(\frac{\alpha^2r^4}{8}-1\right)\cos\left(\alpha+\frac{\alpha r^2}{2}\right)+\frac{4}{\pi\alpha}\cos(r\alpha). \tag{B24}$$

Then

$$I_2\simeq\frac{4}{\lambda R^3|\omega|}\cos\left(\frac{|R_z\omega|}{\lambda}\right), \tag{B25}$$

and

$$I_{3a}\simeq R|\omega|\left(\frac{R_z^2}{\lambda^2R^2}-1\right)\cos\left(R\omega\left[1+\frac{R_z^2}{2\lambda^2R^2}\right]\right)-\left(\frac{\omega^2R_z^4}{8\lambda^4R^2}-1\right)\sin\left(R|\omega|\left[1+\frac{R_z^2}{2\lambda^2R^2}\right]\right), \tag{B26}$$

$$I_{3b}\simeq R|\omega|\left(\frac{R_z^2}{\lambda^2R^2}-1\right)\sin\left(R|\omega|\left[1+\frac{R_z^2}{2\lambda^2R^2}\right]\right)+\left(\frac{\omega^2R_z^4}{8\lambda^4R^2}-1\right)\cos\left(R\omega\left[1+\frac{R_z^2}{2\lambda^2R^2}\right]\right)+\frac{4}{\pi R|\omega|}\cos\left(\frac{|R_z\omega|}{\lambda}\right), \tag{B27}$$

which gives

$$I_3\simeq-\frac{\pi}{\lambda R^2}\left[\exp\left(iR\omega\left[1+\frac{R_z^2}{2\lambda^2R^2}\right]\right)\left[R\omega\left(\frac{R_z^2}{\lambda^2R^2}-1\right)+i\left(\frac{R_z^4\omega^2}{8\lambda^4R^2}-1\right)\right]+\frac{4i}{\pi R|\omega|}\cos\left(\frac{|R_z\omega|}{\lambda}\right)\right]. \tag{B28}$$

Defining $f(R,R_z,\omega)=I_2(R,R_z,\omega)-i\ \mathrm{sgn}(\omega)I_3(R,R_z,\omega)$, we have (summing over valleys) that

$$G_0^{S,P}(\mathbf{R},\omega)\simeq\frac{\sin(\theta_R)}{2\pi^2}\cos\left(K_zR_z\right)\,f(R,R_z,\omega), \tag{B29}$$

$$G_z^{S,P}(\mathbf{R},\omega)\simeq\frac{i\,\cos(\theta_R)}{2\pi^2}\cos\left(K_zR_z\right)\,f(R,R_z,\omega), \tag{B30}$$

with

$$f(R,R_z,\omega)=\frac{1}{\lambda R^2}\left(\frac{4}{R|\omega|}\cos\left(\frac{|R_z\omega|}{\lambda}\right)+i\pi\ \mathrm{sgn}(\omega)\left[\exp\left(iR\omega\left[1+\frac{R_z^2}{2\lambda^2R^2}\right]\right)\left[R\omega\left(\frac{R_z^2}{\lambda^2R^2}-1\right)+i\left(\frac{R_z^4\omega^2}{8\lambda^4R^2}-1\right)\right]\right.\right.$$
$$\left.\left.+\ \frac{4i}{\pi R|\omega|}\cos\left(\frac{|R_z\omega|}{\lambda}\right)\right]\right), \tag{B31}$$

and, for $\omega<0$,

$$f(R,R_z,\omega<0)=-\frac{1}{\lambda R^2}\left(\frac{4}{R\omega}\cos\left(\frac{|R_z|\omega}{\lambda}\right)+i\pi\omega\left[\exp\left(iR\omega\left[1+\frac{R_z^2}{2\lambda^2R^2}\right]\right)\left[R\omega\left(\frac{R_z^2}{\lambda^2R^2}-1\right)+i\left(\frac{R_z^4\omega^2}{8\lambda^4R^2}-1\right)\right]\right.\right.$$
$$\left.\left.+\ \frac{4i}{\pi R\omega}\cos\left(\frac{|R_z|\omega}{\lambda}\right)\right]\right). \tag{B32}$$

Integrating in ω, and to lowest order in $1/R$, one gets

$$\chi^{S,P}_{x,x} \simeq \frac{\omega_F^2}{4\pi^3\lambda^2 R^3}\cos^2(K_z R_z)\cos(2\theta_R)\cos\left(2R\omega_F\left[1+\frac{R_z^2}{2\lambda^2R^2}\right]\right), \tag{B33}$$

$$\chi^{S,P}_{z,z} \simeq -\frac{\omega_F^2}{4\pi^3\lambda^2 R^3}\cos^2(K_z R_z)\cos\left(2R\omega_F\left[1+\frac{R_z^2}{2\lambda^2R^2}\right]\right), \tag{B34}$$

$$\chi^{S,P}_{x,y} \simeq -\frac{\omega_F^2}{4\pi^3\lambda^2 R^3}\cos^2(K_z R_z)\sin(2\theta_R)\cos\left(2R\omega_F\left[1+\frac{R_z^2}{2\lambda^2R^2}\right]\right). \tag{B35}$$

[1] Z. K. Liu, B. Zhou, Y. Zhang, Z. J. Wang, H. M. Weng, D. Prabhakaran, S.-K. Mo, Z. X. Shen, Z. Fang, X. Dai, Z. Hussain, and Y. L. Chen, Science **343**, 864 (2014).

[2] S. K. Kushwaha, J. W. Krizan, B. E. Feldman, A. Gyenis, M. T. Randeria, J. Xiong, S.-Y. Xu, N. Alidoust, I. Belopolski, T. Liang, M. Zahid Hasan, N. P. Ong, A. Yazdani, and R. J. Cava, APL Mater. **3**, 041504 (2015).

[3] Z. K. Liu, J. Jiang, B. Zhou, Z. J. Wang, Y. Zhang, H. M. Weng, D. Prabhakaran, S.-K. Mo, H. Peng, P. Dudin, T. Kim, M. Hoesch, Z. Fang, X. Dai, Z. X. Shen, D. L. Feng, Z. Hussain, and Y. L. Chen, Nat. Mater. **13**, 677 (2014).

[4] H. Yi, Z. Wang, C. Chen, Y. Shi, Y. Feng, A. Liang, Z. Xie, S. He, J. He, Y. Peng, X. Liu, Y. Liu, L. Zhao, G. Liu, X. Dong, J. Zhang, M. Nakatake, M. Arita, K. Shimada, H. Namatame, M. Taniguchi, Z. Xu, C. Chen, X. Dai, Z. Fang, and X. J. Zhou, Sci. Rep. **4**, 6106 (2014).

[5] M. Neupane, S.-Y. Xu, R. Sankar, N. Alidoust, G. Bian, C. Liu, I. Belopolski, T.-R. Chang, H.-T. Jeng, H. Lin, A. Bansil, F. Chou, and M. Z. Hasan, Nat. Commun. **5**, 3786 (2014).

[6] Q. D. Gibson, L. M. Schoop, L. Muechler, L. S. Xie, M. Hirschberger, N. P. Ong, R. Car, and R. J. Cava, Phys. Rev. B **91**, 205128 (2015).

[7] S.-Y. Xu, I. Belopolski, N. Alidoust, M. Neupane, G. Bian, C. Zhang, R. Sankar, G. Chang, Z. Yuan, C.-C. Lee, S.-M. Huang, H. Zheng, J. Ma, D. S. Sanchez, B. Wang, A. Bansil, F. Chou, P. P. Shibayev, H. Lin, S. Jia, and M. Z. Hasan, Science **349**, 613 (2015).

[8] B. Q. Lv, N. Xu, H. M. Weng, J. Z. Ma, P. Richard, X. C. Huang, L. X. Zhao, G. F. Chen, C. E. Matt, F. Bisti, V. N. Strocov, J. Mesot, Z. Fang, X. Dai, T. Qian, M. Shi, and H. Ding, Nat. Phys. **11**, 724 (2015).

[9] B. Q. Lv, H. M. Weng, B. B. Fu, X. P. Wang, H. Miao, J. Ma, P. Richard, X. C. Huang, L. X. Zhao, G. F. Chen, Z. Fang, X. Dai, T. Qian, and H. Ding, Phys. Rev. X **5**, 031013 (2015).

[10] S.-Y. Xu, N. Alidoust, I. Belopolski, Z. Yuan, G. Bian, T.-R. Chang, H. Zheng, V. N. Strocov, D. S. Sanchez, G. Chang, C. Zhang, D. Mou, Y. Wu, L. Huang, C.-C. Lee, S.-M. Huang, B. Wang, A. Bansil, H.-T. Jeng, T. Neupert, A. Kaminski, H. Lin, S. Jia, and M. Zahid Hasan, Nat. Phys. **11**, 748 (2015).

[11] X. Di-Fei, D. Yong-Ping, W. Zhen, L. Yu-Peng, N. Xiao-Hai, Y. Qi, D. Pavel, X. Zhu-An, W. Xian-Gang, and F. Dong-Lai, Chin. Phys. Lett. **32**, 107101 (2015).

[12] A. Principi, G. Vignale, and E. Rossi, Phys. Rev. B **92**, 041107 (2015).

[13] A. K. Mitchell and L. Fritz, Phys. Rev. B **92**, 121109 (2015).

[14] J.-H. Sun, D.-H. Xu, F.-C. Zhang, and Y. Zhou, Phys. Rev. B **92**, 195124 (2015).

[15] M. A. Ruderman and C. Kittel, Phys. Rev. **96**, 99 (1954).

[16] T. Kasuya, Prog. Theor. Phys. **16**, 45 (1956).

[17] K. Yosida, Phys. Rev. **106**, 893 (1957).

[18] S. Saremi, Phys. Rev. B **76**, 184430 (2007).

[19] M. Sherafati and S. Satpathy, Phys. Rev. B **84**, 125416 (2011).

[20] H. Imamura, P. Bruno, and Y. Utsumi, Phys. Rev. B **69**, 121303 (2004).

[21] Z. Wang, Y. Sun, X.-Q. Chen, C. Franchini, G. Xu, H. Weng, X. Dai, and Z. Fang, Phys. Rev. B **85**, 195320 (2012).

[22] D. C. Mattis, *The Theory of Magnetism Made Simple* (World Scientific, Singapore, 2006).

[23] D. N. Aristov, Phys. Rev. B **55**, 8064 (1997).

[24] K. Momma and F. Izumi, J. Appl. Crystallogr. **44**, 1272 (2011).

[25] For Na_3Bi, the values of the parameters are [21] $C_0 \simeq -0.06$ eV, $C_1 \simeq 8.75$ eVÅ^2, $C_2 \simeq -8.4$ eVÅ^2, $M_0 \simeq -0.09$ eV, $M_1 \simeq -10.64$ eVÅ^2, $M_2 \simeq -10.36$ eVÅ^2, and $A \simeq 2.46$ eVÅ. .

[26] P. Lyu, N.-n. Liu, and C. Zhang, J. Appl. Phys. **102**, 103910 (2007).

[27] A. Schulz, A. De Martino, P. Ingenhoven, and R. Egger, Phys. Rev. B **79**, 205432 (2009).

[28] R. R. Biswas and A. V. Balatsky, Phys. Rev. B **81**, 233405 (2010).

[29] J. Klinovaja and D. Loss, Phys. Rev. B **87**, 045422 (2013).

[30] F. Parhizgar, H. Rostami, and R. Asgari, Phys. Rev. B **87**, 125401 (2013).

[31] D. Mastrogiuseppe, N. Sandler, and S. E. Ulloa, Phys. Rev. B **90**, 161403 (2014).

[32] H.-R. Chang, J. Zhou, S.-X. Wang, W.-Y. Shan, and D. Xiao, Phys. Rev. B **92**, 241103 (2015).

[33] M. V. Hosseini and M. Askari, Phys. Rev. B **92**, 224435 (2015).